Connectome-wide investigation of altered resting-state functional connectivity in war veterans with and without posttraumatic stress disorder

Masaya Misaki[a], Raquel Phillips[a], Vadim Zotev[a], Chung-Ki Wong[a], Brent E. Wurfel[a,b],
Frank Krueger[c], Matthew Feldner[d], Jerzy Bodurka[a,e,*]

[a] Laureate Institute for Brain Research, Tulsa, OK, United States
[b] Laureate Psychiatric Clinic and Hospital, Tulsa, OK, United States
[c] School of Systems Biology, George Mason University, Fairfax, VA, United States
[d] Dept. of Psychological Science, University of Arkansas, Fayetteville, AR, United States
[e] Stephenson School of Biomedical Engineering, University of Oklahoma, Norman, OK, United States

ARTICLE INFO

ABSTRACT

Altered resting-state functional connectivity in posttraumatic stress disorder (PTSD) suggests neuropathology of the disorder. While seed-based fMRI connectivity analysis is often used for the studies, such analysis requires defining a seed location *a priori*, which restricts search scope and could bias findings toward presupposed areas. Recently, a comprehensive exploratory voxel-wise connectivity analysis, the connectome-wide association approach, has been introduced using multivariate distance matrix regression (MDMR) for resting-state functional connectivity analysis. The current study performed a connectome-wide investigation of resting-state functional connectivity for war veterans with and without PTSD compared to non-trauma-exposed healthy controls using MDMR.

Thirty-five male combat veterans with PTSD (unmedicated), 18 male combat veterans without PTSD (veterans control, VC), and 28 age-matched non-trauma-exposed healthy males (NC) participated in a resting-state fMRI scan. MDMR analysis was used to identify between-groups differences in regions with altered connectivity. The identified regions were used as a seed for post-hoc functional connectivity analysis.

The analysis revealed that PTSD patients had hypoconnectivity between the left lateral prefrontal regions and the salience network regions as well as hypoconnectivity between the parahippocampal gyrus and the visual cortex areas. Connectivity between the ventromedial prefrontal cortex and the middle frontal gyrus and between the parahippocampal gyrus and the anterior insula were negatively correlated with PTSD symptom severity. VC subjects also had altered functional connectivity compared to NC, including increased connectivity between the posterior insula and several brain regions and decreased connectivity between the precuneus region and several other brain areas.

The decreased connectivity between the lateral prefrontal regions and the salience network regions in PTSD was consistent with previous reports that indicated lowered emotion-regulation function in these regions. The decreased connectivity between the parahippocampal gyrus and visual cortex supported the dual representation theory of PTSD, which suggests dissociation between sensory and contextual memory representations in PTSD. The theory also supposes that the precuneus is a region that triggers retrieval of sensory memory of traumatic events. The decreased connectivity at the precuneus for VC might be associated with suppressing such a process.

1. Introduction

Posttraumatic stress disorder (PTSD) is one of the most prevalent mental disorders for war veterans. A screening for mental health problems by the US military suggested 9.8% of veterans returning from Iraq, 4.7% from Afghanistan, and 2.1% from other locations were at risk of PTSD (Hoge et al., 2006). Several studies have suggested a biological basis for PTSD (Pitman et al., 2012 for review), including neuroimaging studies (e.g., Hayes et al., 2012; Lanius et al., 2006; Liberzon and Sripada, 2008; Patel et al., 2012). Nonetheless, ongoing research is needed to better understand the complex neurobiological abnormalities that underlie this costly and chronic condition.

One of the types of neuroimaging studies that is providing abundant insights into the neuropathology of intrinsic brain activity in PTSD is

---

resting-state functional magnetic resonance imaging (rsfMRI), which measures blood oxygenation level dependent (BOLD) signal while a subject does not perform any explicit task. This includes studies using voxel-wise resting-state signal measurement such as amplitude of low-frequency fluctuation (ALFF) (Zou et al., 2008) and regional homogeneity (ReHo) (Zang et al., 2004). Meta-analyses of these studies combined with positron emission tomography (PET) studies (Koch et al., 2016; Wang et al., 2016) showed that PTSD patients had increased resting-state signal fluctuation or activity in the amygdala and the parahippocampal gyrus and decreased fluctuation or activity in the superior frontal gyrus and the middle frontal gyrus, although there is significant variability across studies. Decomposition of spatial coactivation patterns, such as independent component analysis (ICA), was also used in an rsfMRI study (Calhoun and Adali, 2012). Although ICA is typically employed to extract the spatial pattern of a functional network, it can also be used to evaluate connectivity with a dual regression technique (Filippini et al., 2009), in which correlations between the global network (independent component) time-course and voxel-wise time-courses are examined. Tursich et al. (2015) indicated that the connectivity of the salience network (SN) with the posterior insula and the superior temporal gyrus were negatively correlated with hyperarousal symptoms in PTSD. Graph analysis for resting-state connectivity (Fornito et al., 2013) was also employed in an rsfMRI study of PTSD (Lei et al., 2015), indicating that the resting-state functional network for PTSD shifted toward small-worldization with increased centrality in the default-mode network (DMN) and the SN.

Another commonly employed measure of rsfMRI is functional connectivity (Friston, 1994), which evaluates the correlation of signal time-courses between a seed region and other brain regions. Seed-based connectivity analyses also showed aberrant resting-state connectivity for PTSD. Brown et al. (2014) indicated increased connectivity between the basolateral amygdala and the anterior cingulate cortex (ACC), dorsal ACC, and dorsomedial prefrontal cortex as well as decreased connectivity between the amygdala and the left inferior frontal gyrus for PTSD patients compared to trauma-exposed controls. Zhang et al. (2016) found decreased connectivity between the ventral anterior insula and the ACC, and between the right posterior insula and the left inferior parietal lobe and the postcentral gyrus. Kennis et al. (2015) showed decreased connectivity between the caudal ACC and the precentral gyrus and between the perigenual ACC and the superior medial frontal gyrus and middle temporal gyrus.

These findings suggest several converging regions of pathological resting-state activity or connectivity for PTSD such as hyperactivity and increased connectivity in the SN regions, including the amygdala, anterior insula, and ACC, and hypoactivity and decreased connectivity in the prefrontal emotion-regulation areas including lateral prefrontal regions and dorsal and ventral medial prefrontal regions. Deficits in emotion regulation function due to hyperactive and hyperconnected SN and its hypoconnectivity with lateral prefrontal regions are thought to underlie the hyperarousal symptoms of PTSD (Fonzo et al., 2010; Lanius et al., 2006; Zhu et al., 2015).

A limitation of previous functional connectivity studies, however, is that seed-based resting-state connectivity analysis requires the a priori definition of a seed location. This restricts the scope of investigation to relations with the presupposed seed area and could bias findings toward the seed area. In particular, a priori predictions about the functioning of regions implicated in emotion regulation may have resulted in the over-representation of these regions in our current understanding of resting state functional connectivity in PTSD. Indeed, abnormal brain functioning in PTSD is not limited to the emotion regulation network. Task-based fMRI studies have suggested abnormal functioning in regions implicated in attention and working memory (Aupperle et al., 2012) as well as memory representation (Brewin, 2011; Whalley et al., 2013), such as the medial temporal and posterior brain regions including hippocampal, parietal, and occipital areas. Those low-level sensorimotor regions are rarely identified as seeds for functional connectivity

analyses in studies of PTSD. While voxel-wise whole-brain investigations of resting-state activity with ALFF, ReHo, and PET (Bonne et al., 2003; Kohn et al., 2014; Wang et al., 2016) often suggested altered resting-state activity in the sensorimotor, visual cortex, and hippocampal/parahippocampal areas, these measures did not elucidate functional connectivity of the regions. Connectivity analysis using ICA also does not capture region-by-region functional connectivity. Instead, it analyzes connectivity between a global brain network and a voxel-wise signal.

To complement these analyses, and to resolve the limitation of seed-based connectivity analysis, yet another rsfMRI analysis has been proposed: a connectome-wide approach that investigates comprehensive voxel-wise connectivity alterations (Shehzad et al., 2014). This approach utilizes a multivariate distance matrix regression (MDMR) analysis (Anderson, 2001) and can examine voxel-wise connectivity alterations in the whole brain without a priori seed definition. Satterthwaite et al. (2015) applied this analysis to major depressive disorder (MDD), PTSD, and female healthy control subjects and found that decreased connectivity between the amygdala and the dorsolateral prefrontal cortex, ACC, and anterior insula correlated with depression symptom severity. They also showed that elevated connectivity between the amygdala and the ventromedial prefrontal cortex correlated with anxiety symptom severity.

The aim of this study was to examine altered resting-state connectivity of male war veterans with and without PTSD and male age-matched non-trauma-exposed healthy controls using a connectome-wide approach. We expected connectome-wide investigation of altered resting-state functional connectivity to reveal a comprehensive view of the neuropathology of intrinsic brain functional connectivity among people with PTSD without bias introduced via hypothesis testing.

In addition to examining veterans with combat-related PTSD, we also examined altered resting-state connectivity among combat veterans without PTSD. While a population with trauma experience without PTSD has often been considered a control group for understanding atypical functioning among people with PTSD, several studies have demonstrated atypical brain activation in this group compared to non-trauma-exposed people. For example, war-deployed soldiers who did not develop PTSD showed lowered midbrain activation in a working memory task and decreased connectivity between the midbrain region and the prefrontal cortex compared to non-deployed soldiers (van Wingen et al., 2012). Meta-analysis of region-wise resting-state brain activation (Patel et al., 2012) indicated higher prefrontal activity among trauma-exposed people without PTSD compared to non-trauma-exposed controls. A resting-state functional connectivity analysis with an ACC seed (Kennis et al., 2015) also indicated that war veterans without PTSD had a different pattern of resting-state connectivity compared to civilian controls. The differences include decreased connectivity between the caudal ACC and the precentral gyrus and between the perigenual ACC and the superior medial frontal and the middle temporal gyrus, and increased connectivity between the rostral ACC and precentral and middle frontal regions. These data suggest that war veterans without PTSD could have altered intrinsic brain activation compared to both people with PTSD and non-trauma-exposed controls. Importantly, altered brain functioning in PTSD and trauma-exposed controls may not be incremental. Trauma-exposed controls without PTSD could have a specific brain alteration that does not exist in PTSD, which may function as an adaptive change to trauma exposure or as a protective factor that reduces the likelihood of developing PTSD subsequent to trauma exposure. The current study, therefore, employed three groups of male subjects: war veterans with PTSD (unmedicated), war veterans without PTSD, and age-matched non-trauma-exposed healthy controls. The study examined comprehensive connectome-wide differences in resting-state functional connectivity between these groups.

Table 1

Demographic characteristics of war veterans with PTSD, war veterans without PTSD (veteran controls; VC), and non-trauma-exposed healthy controls (NC). CAPS score was not available for two PTSD and two VC subjects. PCL-M score was not available for one PTSD and two VC subjects. MADRS score was not available for one PTSD and one VC subjects. Mean ± SD for each group and statistics for the difference between the groups are shown except for age and head motion. Both age and head motion were not significantly different between groups with ANOVA ($F(2,78) = 1.39$, $p = 0.260$ for age and $F(2,78) = 1.29$, $p = 0.281$ for motion).

	PTSD	VC	NC	PTSD - VC	PTSD – NC	VC - NC
Number of participants	35	18	28			
Age	31.9 ± 7.1	33.4 ± 9.5	29.0 ± 11.0			
(range)	21–48	22–55	19–53			
CAPS	55.2 ± 18.4	4.8 ± 4.9	NA	$t(47) = 10.73$ $p < 0.001$		
PCL-M	48.0 ± 14.2	19.6 ± 2.6	NA	$t(48) = 7.87$ $p < 0.001$		
MADRS	20.4 ± 9.6	1.4 ± 1.8	1.5 ± 1.9	$t(76) = 9.87$ $p < 0.001$	$t(76) = 11.43$ $p < 0.001$	$t(76) = -0.04$ $p = 0.999$
HAM-A	18.2 ± 7.8	1.9 ± 1.5	2.2 ± 2.5	$t(76) = 10.17$ $p < 0.001$	$t(76) = 11.67$ $p < 0.001$	$t(76) = 0.14$ $p = 0.989$
Motion (average FD)	0.06 ± 0.03	0.07 ± 0.02	0.05 ± 0.02			

Abbreviations: CAPS: Clinician-Administered PTSD Scale, PCL-M: PTSD Checklist - military version, MADRS: Montgomery-Asberg Depression Scale, HAM-A: Hamilton Anxiety Rating Scale, FD: frame-wise displacement of fMRI images (mm/volume), NA: not available.

2. Material and methods

2.1. Participants

Thirty-nine male combat veterans with PTSD and 22 male combat veterans without PTSD (veterans control, VC) participated in the resting-state fMRI scan as part of a neurofeedback training study (to be published separately). In addition, 28 age-matched non-trauma-exposed healthy males who had participated in another study (Misaki et al., 2016) were employed as non-trauma-exposed healthy controls (NC). Four PTSD and 4 VC participants were excluded from the analysis due to excessive head motion (> 40 censored time points, see below). Table 1 shows numbers of analyzed participants and mean ages for each group. There was no significant age difference between the groups. The study was approved by the Western Institutional Review Board, Puyallup, WA. All procedures with human subjects were conducted according to the code of ethics of the World Medical Association (Declaration of Helsinki) for experiments involving humans. All subjects gave written informed consent to participate in the study and received financial compensation.

The psychiatric diagnosis was established according to Diagnostic and Statistical Manual of Mental Disorders, Fourth Edition, Text Revision (American Psychiatric Association, 2000) criteria using both the Structured Clinical Interview for DSM-IV Disorders (First et al., 1996) administered via a trained clinical interviewer and an unstructured interview with a psychiatrist. Exclusion criteria included serious suicidal ideation, psychosis, major medical or neurological disorders, general MRI exclusions, and exposure to psychotropic medications or to any medication likely to influence cerebral function or blood flow within three weeks (8 weeks for fluoxetine). Two VC subjects endorsed a history of alcohol abuse, one VC subject endorsed a history of alcohol dependence, one VC subject endorsed a history of major depressive disorder (MDD), and one VC subject endorsed a history of alcohol abuse and major depressive disorder. These morbidities for VC were fully remitted at study time. Additional exclusion criteria applied to the NC were history of war deployment or current or past personal or family (i.e., first-degree relative) history of axis I psychiatric conditions, as assessed using the Family Interview for Genetics Studies (FIGS).

2.2. Symptom measurement

PTSD symptoms were measured with the Clinician-Administered PTSD Scale (CAPS) for DSM-IV (Blake et al., 1995) and the PTSD Checklist - Military Version (PCL-M) (Weathers et al., 1993). The CAPS is a well-established semi-structured clinical interview that is used to determine the presence of traumatic event exposure, characteristics of the traumatic event, and frequency and severity of PTSD symptoms and diagnoses. The CAPS has excellent psychometric properties including convergent and discriminant validity, test-retest and interrater reliability, and internal consistency (Weathers et al., 2001). The CAPS was administered by research staff trained to mastery in administration of the interview. The PCL-M is a 17-item questionnaire that was used to measure DSM-IV-defined PTSD symptom severity (American Psychiatric Association, 2000). Subjects indicate the degree to which they have been bothered by each symptom in the past week on a 1 (*not at all bothered*) to 5 (*extremely bothered*) scale. The PCL-M has shown strong convergent and divergent validity (Blanchard et al., 1996; Ruggiero et al., 2003).

Depression and anxiety symptoms were also measured with the Montgomery-Asberg Depression Rating Scale (MADRS) (Montgomery and Asberg, 1979) and the Hamilton Anxiety Scale (HAM-A) (Hamilton et al., 1976), respectively. The MADRS and HAM-A are well-established measures of the severity of depressive symptoms and anxiety symptoms with adequate psychometric properties (Jiang and Ahmed, 2009; Maier et al., 1988; Montgomery and Asberg, 1979; Reimherr et al., 2010). Table 1 includes mean symptom scores for each group.

2.3. MRI measurement

The resting-state session took place prior to any task sessions. During the resting-state fMRI, participants were instructed not to move and to relax and rest while looking at a fixation cross on the screen. Magnetic resonance imaging was conducted on a whole-body 3 T MR750 MRI scanner (GE Healthcare, Milwaukee, WI) equipped with 32-channel receive-only head array coils (GE Healthcare, Nova Medical, Wilmington, MA). A single-shot gradient-recalled echo-planner imaging (EPI) sequence with sensitivity encoding (SENSE) was used for fMRI. In the study for veterans, the EPI imaging parameters were TR = 2000 ms, TE = 30 ms, FA = 90°, FOV = 240 mm, 34 axial slices with 2.9 mm thickness with 0.5 mm gap, matrix = 96 × 96, SENSE acceleration factor $R = 2$. The EPI images were reconstructed into a 128 × 128 matrix resulting 1.875 × 1.875 × 3.4 mm³ voxel volume. The resting fMRI run time was 6 min 50 s (205 volumes). In the study for NC subjects, the EPI imaging parameters were TR = 2000 ms, TE = 25 ms, FA = 75°, FOV = 240 mm, 34 axial slices with 2.9 mm thickness without gap, matrix = 96 × 96, SENSE acceleration factor $R = 2$. The EPI images were reconstructed into a 128 × 128 matrix resulting in 1.875 × 1.875 × 2.9 mm³ voxel volume. The resting fMRI run time was 7 min 30 s (225 volumes). We used only the first 205
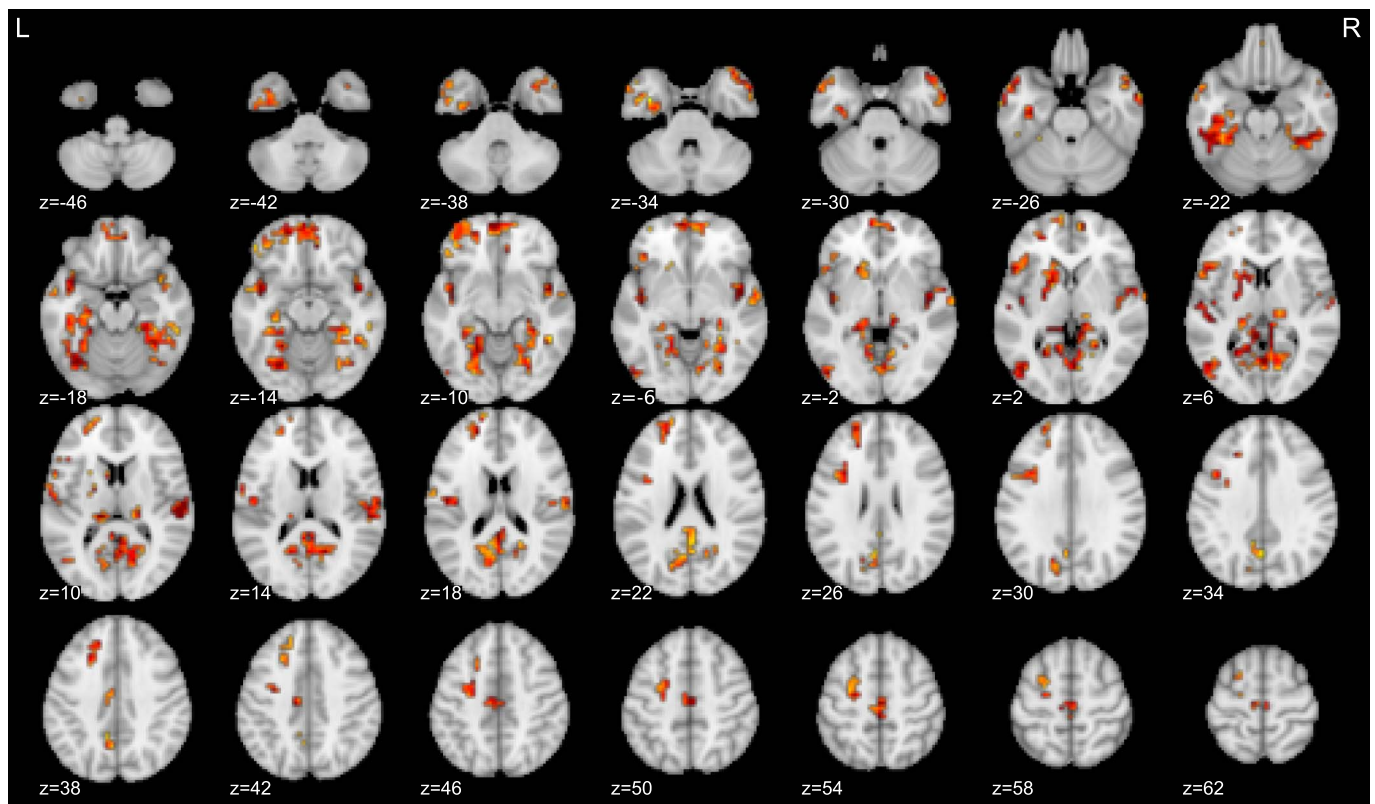
Fig. 1. MDMR pseudo-F value map for the main effect of groups (PTSD, VC, NC) thresholded with voxel-wise $p < 0.005$ and cluster-size $p < 0.05$.

volumes for the analysis to equate the number of volumes between the studies. Physiological pulse oximetry and respiration waveforms were simultaneously recorded (40 Hz) in both studies. A photoplethysmograph with an infrared emitter placed under the pad of a participant's finger was used for pulse oximetry, and a pneumatic respiration belt was used for respiration measurements.

To provide anatomical reference for fMRI data, T1-weighted MRI images were acquired with a magnetization-prepared rapid gradient-echo (MPRAGE) sequence. The following parameters were used: FOV = 240 × 192 mm, matrix = 256 × 256, 120 axial slices, slice thickness = 0.9 mm, $0.9375 \times 0.9375 \times 0.9$ mm^3 voxel volume, TR = 5 ms, TE = 2.0 ms, $R = 2$, flip angle = 8°, delay time = 1400 ms, inversion time = 725 ms, sampling bandwidth = 31.2 kHz, scan time = 5 min 40 s.

2.4. MRI image processing

Analysis of Functional NeuroImages (AFNI) software (http://afni.nimh.nih.gov/afni/) was used for imaging analysis. We utilized the afni_proc.py command to make a data processing script and used default parameters of this command except where noted. Initial five volumes were excluded from analysis. Outlier time points were replaced with interpolation (despike). RETROICOR (Glover et al., 2000) was applied to remove respiration- and cardiac-induced noise in the BOLD signal. Physiological fluctuations correlated with low-frequency changes in respiration depth were regressed out from the BOLD signal using respiration volume per time (RVT) correction (Birn et al., 2008). Slice-timing differences were corrected by aligning to the first slice. Motion correction was applied by aligning all functional volumes to the first volume. Nonlinear warping to the MNI template brain with resampling to 2 mm^3 voxels was done with the Advanced Normalization Tools (ANTs) software (Avants et al., 2008) (http://stnava.github.io/ANTs/). We used the non-linearly aligned and averaged MNI152 brain provided with the FSL package (https://fsl.fmrib.ox.ac.uk/fsl/fslwiki)

as a template. Spatial smoothing (4 mm FWHM) and scaling to percent change were applied to the data.

Further noise reduction was applied by regressing out three principal components of the ventricle signal, local white matter average signal (ANATICOR) (Jo et al., 2010), 12 motion parameters (3 shift and 3 rotation parameters with their temporal derivatives), and low-frequency fluctuation (3rd-order polynomial model) from the signal time course. White matter and ventricle masks were extracted using Free-Surfer 5.3 (http://surfer.nmr.mgh.harvard.edu/) from the anatomical image of individual subject and then warped to the normalized fMRI image space. Any fMRI time point with large motion (> 0.25 mm frame-wise displacement (FD)) along with the following point was censored within the regression (Power et al., 2015). FD was calculated as the root sum of squared temporal differences of six motion parameters.

2.5. Effect of scan parameter difference

Since fMRI scan parameters between the veteran groups (PTSD and VC) and the NC group were different, we examined signal difference between the groups specifically in their spatial smoothness and temporal signal to noise ratio (TSNR). It has been indicated that variable spatial smoothness and TSNR are major sources of inter-scanner variability in activation estimation of fMRI (Friedman and Glover, 2006; Friedman et al., 2006). We reasoned that if these properties were similar between the groups, connectivity difference between the groups could not be attributed to scan parameters difference. Spatial smoothness was evaluated using AFNI 3dFWHMx for the processed image after noise components were regressed out. Smoothness estimates were restricted to brain voxels that were covered by all subjects and censored volumes were excluded from the estimation. TSNR was defined as the mean signal divided by the temporal standard deviation for each voxel. TSNR was calculated for functional images before applying regression and censored volumes were excluded. We used the median TSNR in

Table 2

Peak locations of significant clusters for the main effect of groups in the MDMR analysis. Local maximum positions at least 30 mm apart from each other were extracted from significant clusters. Cluster-size p-values were evaluated by permutation test with 10,000 random permutations.

Peak location (MNI, mm)			Brain region	Pseudo-F	Cluster size (4 mm^3 voxel)	Cluster-size p-value
x	y	z				
12	−28	−2	R Thalamus	2.545	520	0.0001
−28	−68	−14	L Fusiform	2.377		
4	−68	2	R Lingual	2.335		
−36	−16	−26	L Parahippocampal	2.18		
44	−40	−22	R Fusiform	2.176	146	0.0014
24	−52	2	R Parahippocampal	1.915		
−4	60	−10	L vmPFC (BA11)	2.341	127	0.0020
−20	48	18	L Superior Frontal (BA10)	2.077	54	0.0100
−16	12	6	L Lentiform Nucleus	2.188		
−8	−20	62	L SMA	2.252	50	0.0120
56	4	−34	R Middle Temporal	2.171	49	0.0124
−44	−8	−6	L Insula	3.564	48	0.0126
−24	0	46	L Middle Frontal (BA6)	2.083	46	0.0138
−52	20	2	L Inferior Frontal (BA47)	2.088	44	0.0155
56	−24	10	R Transverse Temporal (BA41)	2.937	41	0.0173
−52	−76	−6	L Inferior Temporal/ Middle Occipital	2.216	38	0.0211
44	−8	−2	R Insula	2.69	36	0.0236
−48	−24	6	L Superior Temporal	2.177	34	0.0252
−32	12	26	L Middle Frontal (BA44)	1.988	30	0.0330
−52	8	−26	L Middle Temporal	2.051	28	0.0382
56	0	2	R Superior Temporal	1.984	26	0.0438
−24	28	34	L Superior Frontal (BA9)	1.927	26	0.0438

Abbreviations: L: left, R: right, BA: Brodmann area, vmPFC: ventromedial prefrontal cortex, SMA: supplementary motor area.

gray matter voxels. Friedman and Glover (2006) indicated that by covarying this measure during regression analysis one could eliminate significant effect of inter-scanner variability on activation estimation. We used Welch's two-tailed t-test to examine group difference of the mean smoothness in x, y, and z directions and the median TSNR in gray matter voxels.

2.6. MDMR analysis

MDMR analysis (Anderson, 2001; Shehzad et al., 2014) was applied to investigate comprehensive voxel-wise resting-state connectivity alteration between PTSD, VC, and NC groups. The processed resting-state fMRI image was down-sampled to 4 mm^3 voxels. In order to avoid mixing noise outside the brain, we applied an anatomical brain mask to the functional image before resampling. Since we had already applied local white matter signal and ventricle signal regression at preprocessing, masking these regions was not applied at resampling. This down-sampling process was necessary because the whole-brain voxel-wise connectivity matrix in the original resolution was computationally too large for current hardware. To further reduce data size, only the voxels in gray matter regions were extracted from the down-sampled image. The gray matter mask was extracted from the MNI152 template brain provided with FSL. This masking resulted in extracting 18,693 voxels that were subject to the MDMR analysis.

We followed the procedure introduced in Shehzad et al. (2014) for the MDMR analysis, which is briefly reproduced here. MDMR is a mass voxel-wise analysis as it is performed for each voxel independently. Unlike a seed-based analysis that has many correlation statistics for one voxel, MDMR has a single multivariate omnibus statistic for each voxel.

In each voxel, a connectivity map from that voxel to all other voxels was made with Pearson's correlations between signal time-courses of the voxels. The dependent variable of MDMR is a distance matrix of the connectivity maps between subjects. The distance of the maps between subject i and j, (d_{ij}) was calculated with Euclidean distance of Fisher's z-transformed connectivity maps. The MDMR analysis evaluates the association between the distance matrix (dissimilarities of connectivity maps across subjects) and the predictor variables in the design matrix, X, using a pseudo-F value statistic, $F = \frac{tr(HG)/(m-1)}{tr[(I-H)G]/(n-m)}$, where $H = X(X^TX)^{-1}X^T$ is the hat matrix that maps response values (G) to the fitted value space, m is the number of columns in X, and tr is the trace of matrix. G is the mean-centered distance matrix as $G = CAC$, where $C = \left(I - \frac{1}{n}11^T\right)$, $A = \left(-\frac{1}{2}d_{ij}^2\right)$, n is the number of subjects, I is the $n \times n$ identity matrix and 1 is a vector of n 1 s. In the current study, the design matrix X included two columns of group factors for PTSD and VC, in which 1 indicated PTSD and 0 others, and 1 indicated VC and 0 others, respectively. This coding means that NC is a reference group and the effects of PTSD and VC relative to NC were evaluated. X also included columns of age and motion size (average FD) as nuisance variables as well as all 1 s for the intercept.

Individual effect of regressors was estimated using a partial design matrix. Hat matrix with effects of no interest regressors was subtracted from the full hat matrix as $H_I = H - H_N$, where $H_N = X_N(X_N^TX_N)^{-1}X_N^T$, and X_N is a design matrix only with age, motion, and intercept columns. Pseudo-F value for the sum of the effect of interest, namely the main effect of the group difference, was then calculated as $F_I = \frac{tr(H_IG)/(m_I)}{tr[(I-H)G]/(n-m)}$, where m_I (= 2) is the number of effect of interest regressors.

Statistical tests for the pseudo-F value were performed with a permutation test. Nuisance regressors in the permutation test need to be handled differently from the regressors of interest because effect of interest should be evaluated after excluding nuisance effects. We used the Smith procedure (Winkler et al., 2014), in which regressors of interest were orthogonalized with regard to nuisance regressors and then the orthogonalized regressors of interest were permuted randomly. 10,000 random permutations were performed in the analysis.

These procedures were repeated for all voxels as a seed, and pseudo-F values (with respective p-values) were mapped onto the brain to make a statistical parametric map. We used a computationally efficient method introduced by Shehzad et al. (2014), in which evaluations for all voxels of all permutations were performed in one-time matrix multiplication. The MDMR statistical map was thresholded with voxel-wise $p < 0.005$, and then with cluster-size corrected $p < 0.05$. Cluster-size corrected p-value was evaluated with the same permutation procedure as the voxel-wise evaluation to avoid inflated false positive rate (Eklund et al., 2016).

2.7. Post-hoc seed-based analysis

MDMR statistical map indicates that a whole-brain connectivity pattern at a voxel is altered between the groups. However, it does not show which specific connectivity is altered. To elucidate which voxel-by-voxel connectivity was altered between the groups, post-hoc seed-based connectivity analysis was performed for the significant regions of the MDMR statistical map. Note that this analysis was performed only for a post-hoc investigation and restricted to the regions with significant MDMR statistics so that we could avoid multiple testing problems across seed-based analyses that could arise if we picked arbitrary regions for seed-based analysis.

The post-hoc analysis was performed with the original resolution whole-brain functional images (not restricted to gray matter). Seed regions were placed at peak locations of the significant clusters in the MDMR statistical map of the group main effect. Peak coordinates in each significant cluster separated by at least 30 mm were extracted. Seed area was a 6 mm-radius sphere centered at the peak coordinates of
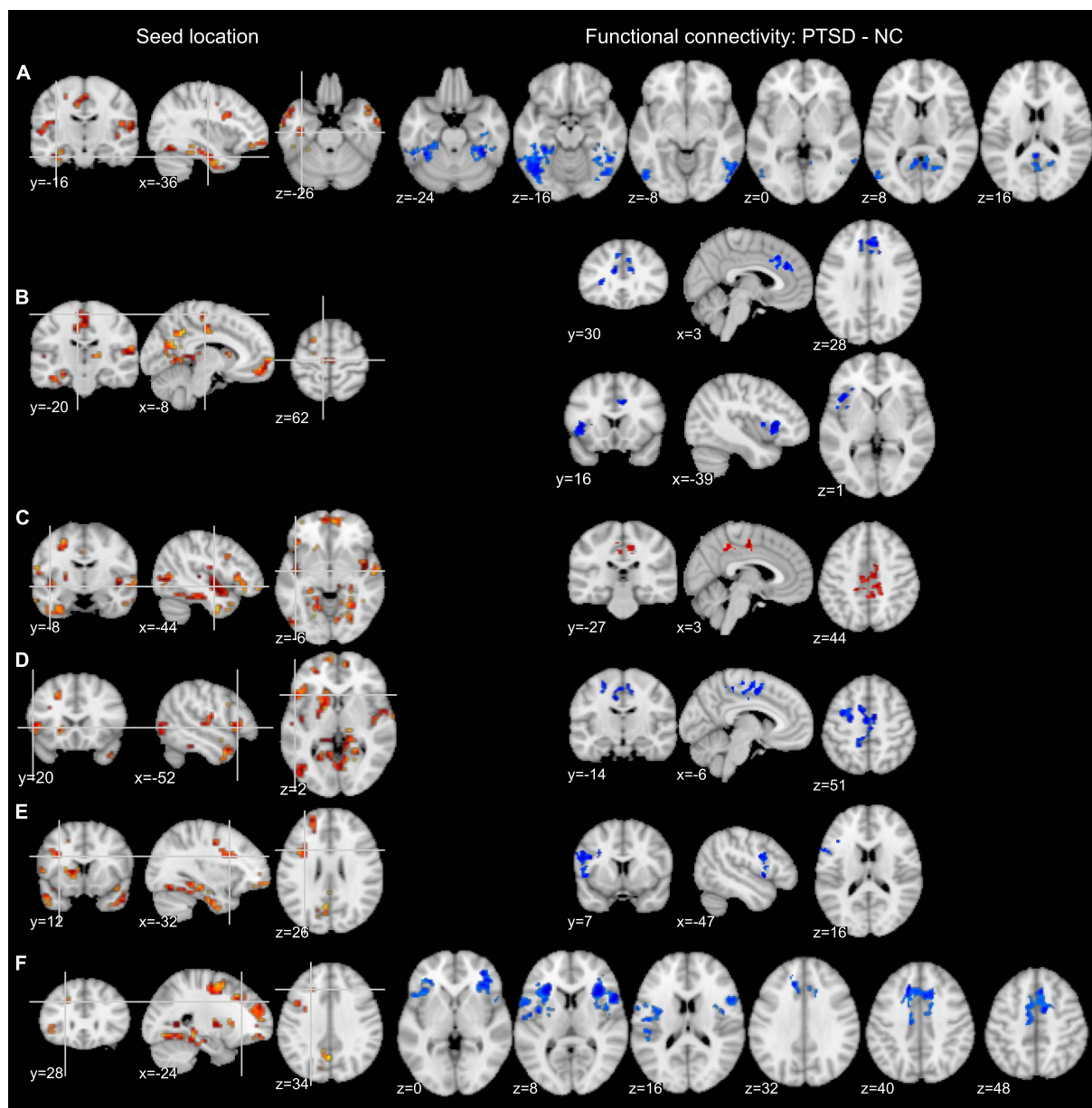
Fig. 2. Seed locations (indicated by crosshair) on the MDMR statistical map (left) and *t*-value maps of the regions with significantly (voxel-wise $p < 0.005$ and cluster-size-corrected $p < 0.016$) altered connectivity (right) for PTSD compared to NC (non-trauma-exposed controls) in post-hoc analysis. Connectivity alteration for PTSD was found for seed locations at the left parahippocampal gyrus (A), left SMA (supplementary motor area) (B), left insula (C), left inferior frontal gyrus (D), left middle frontal gyrus (E), and left superior frontal gyrus (E).

the MDMR statistical map. Average signal time-course of the seed area was used as a reference signal to calculate correlations with other voxels. Fisher's z-transformation was applied to the correlation coefficient to make a connectivity map for each subject. Voxel-wise general linear model analysis was performed for the connectivity map with the same design matrix as the MDMR analysis. *t*-value maps of each group contrast, PTSD-NC, VC-NC, and PTSD-VC, were calculated and thresholded with voxel-wise $p < 0.005$ and cluster-size corrected $p < 0.016$ for multiple testing of three groups. Cluster-size corrected *p*-value was evaluated with the permutation test (10,000 permutations) using the Smith procedure (Winkler et al., 2014).

3. Results

CAPS, PCL-M, MADRS and HAM-A were significantly higher for the PTSD group compared to the VC and NC groups, and not significantly different between the VC and NC groups. Amount of head motion

(average FD) was not significantly different between groups (Table 1). Spatial smoothness and TSNR of functional images were not significantly different between the veterans and NC groups. Mean spatial smoothness was 5.28 mm for veterans and 5.27 mm for NC ($t(56.859)$ = 0.331, $p = 0.742$). Mean gray matter median TSNR was 127.2 for veterans and 123.3 for NC ($t(56.915) = 0.64$, $p = 0.525$).

Fig. 1 shows the thresholded map of pseudo-*F* value for the main effect of group in the MDMR analysis. Peak locations of the clusters with significant effect (cluster-size $p < 0.05$) are shown in Table 2. These peak locations were used as seeds for post-hoc seed-based connectivity analysis.

Fig. 2 shows seed locations and regions with significant functional connectivity alteration for the PTSD compared to NC groups. Supplementary table S1 shows peak locations in significant clusters of altered connectivity in PTSD–NC comparison at post-hoc analysis. Significantly decreased connectivity for PTSD was seen between the left parahippocampal seed and the bilateral fusiform gyrus, middle occipital,
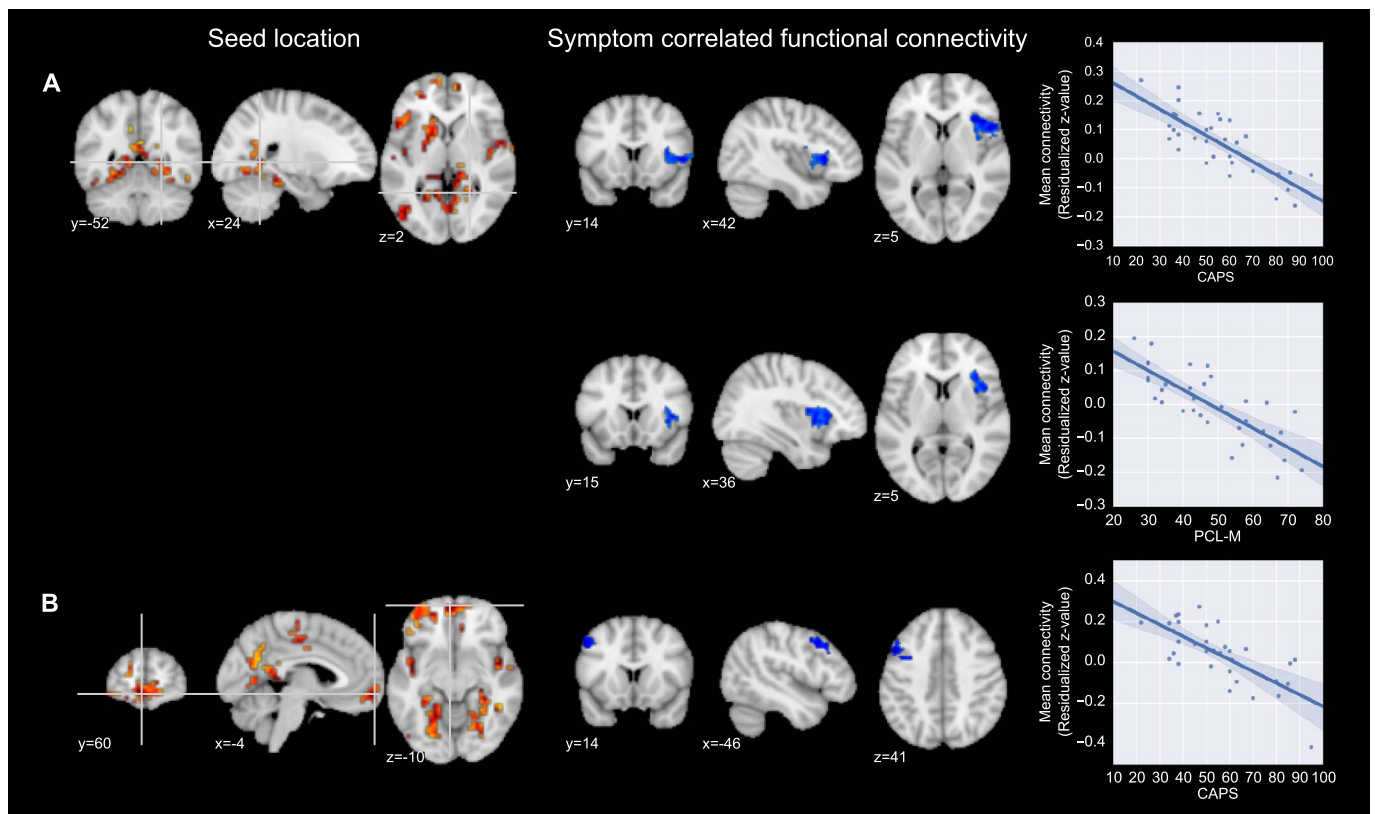
Fig. 3. Seed locations (indicated by crosshair) on the MDMR statistical map (left) and *t*-value maps of the regions with significant symptom-correlated connectivity (middle) among subjects with PTSD (voxel-wise $p < 0.005$ and cluster-size-corrected $p < 0.05$). Functional connectivity correlated with PTSD symptoms (CAPS and PCL-M) was found for seed locations at the right parahippocampal gyrus (A) and the left ventromedial prefrontal cortex (vmPFC) (B). Right panel shows symptom association with mean connectivity (z-value residualized with regard to age and motion covariates) in the regions shown in the maps (middle) with fitted line and its 95% confidence interval. CAPS: Clinician-Administered PTSD Scale, PCL-M: PTSD Checklist - Military Version.

middle temporal, and the posterior cingulate areas (Fig. 2A). Decreased connectivity for PTSD was also seen between the left medial frontal (supplementary motor area; SMA) seed and the anterior cingulate and the left anterior insula regions (Fig. 2B). Multiple left lateral prefrontal seeds showed decreased connectivity for PTSD including between the left inferior frontal seed and the right SMA and the left middle frontal region (Fig. 2D), between the left middle frontal seed and the left inferior frontal and the left superior temporal regions (Fig. 2E), and between the left superior frontal seed and the SMA, anterior cingulate, anterior insula, and inferior frontal regions (Fig. 2F). These hypo-connected regions (Fig. 2F) overlapped with salience network (SN) regions (Menon and Uddin, 2010). Increased functional connectivity for PTSD was seen between the left insula seed and the right middle cingulate region (Fig. 2C).

Correlations between symptom severity and functional connectivity alterations were also examined among people with PTSD for the seed locations in Table 2. The design matrix of this analysis included symptom scores instead of the group factor, along with age and motion covariates. The same permutation procedure used in the post-hoc analysis of group comparisons was used here. Fig. 3 shows seed locations and regions with connectivity significantly (voxel-wise $p < 0.005$ and cluster-size $p < 0.05$) correlated with PTSD symptom scores (CAPS, PCL-M). Peak locations of the significant clusters in Fig. 3 are shown in Supplementary Table S2. Connectivity between the right parahippocampal seed and the right anterior insula was negatively correlated with CAPS and PCL-M (Fig. 3A). Connectivity between the ventromedial prefrontal cortex (vmPFC) seed and the left middle frontal region was negatively correlated with CAPS scores (Fig. 3B). As a complementary analysis, we also examined the connectivity correlation with depression (MADRS) and anxiety (HAM-A) scores for PTSD

(Supplementary Fig. S1). Similar to CAPS and PCL-M, MADRS and HAM-A were negatively correlated with functional connectivity between the right parahippocampal seed and the right anterior insula (Supplementary Fig. S1A). Additionally, connectivity between the left insula and the left middle frontal gyrus was negatively correlated with MADRS and HAM-A (Supplementary Fig. S1B), and connectivity between the left middle frontal and the right inferior parietal regions was negatively correlated with MADRS scores (Supplementary Fig. S1C).

Fig. 4 shows seed locations and regions with significant functional connectivity alteration in the VC compared to NC group. Supplementary table S3 shows peak locations in significant clusters of altered connectivity in the post-hoc VC–NC comparison. Significantly decreased connectivity for VC was seen between the right lingual seed and the medial prefrontal area (Fig. 4A), between the left superior frontal seed and the posterior default mode network areas including the precuneus, posterior cingulate, and the right inferior parietal regions (Fig. 4B), between the left middle frontal seed and the left postcentral region (Fig. 4D), between the right transverse temporal seed and the precuneus (Fig. 4E), and between the left superior temporal seed and the precuneus (Fig. 4G). Significantly increased connectivity was seen between the left posterior insula seed and the right posterior insula, right lingual, and right cuneus regions (Fig. 4C) and between the left posterior insula and the right postcentral, right middle frontal, right middle temporal, right posterior cingulate, left superior parietal, right inferior frontal, right precuneus, and right thalamus.

No significant connectivity differences between the PTSD and VC groups were found in the post-hoc analysis. This could be due to the presence of remitted morbidities in the VC group, such as alcohol abuse, alcohol dependence, and major depressive disorder. We examined associations of these morbidity histories in the VC group with the
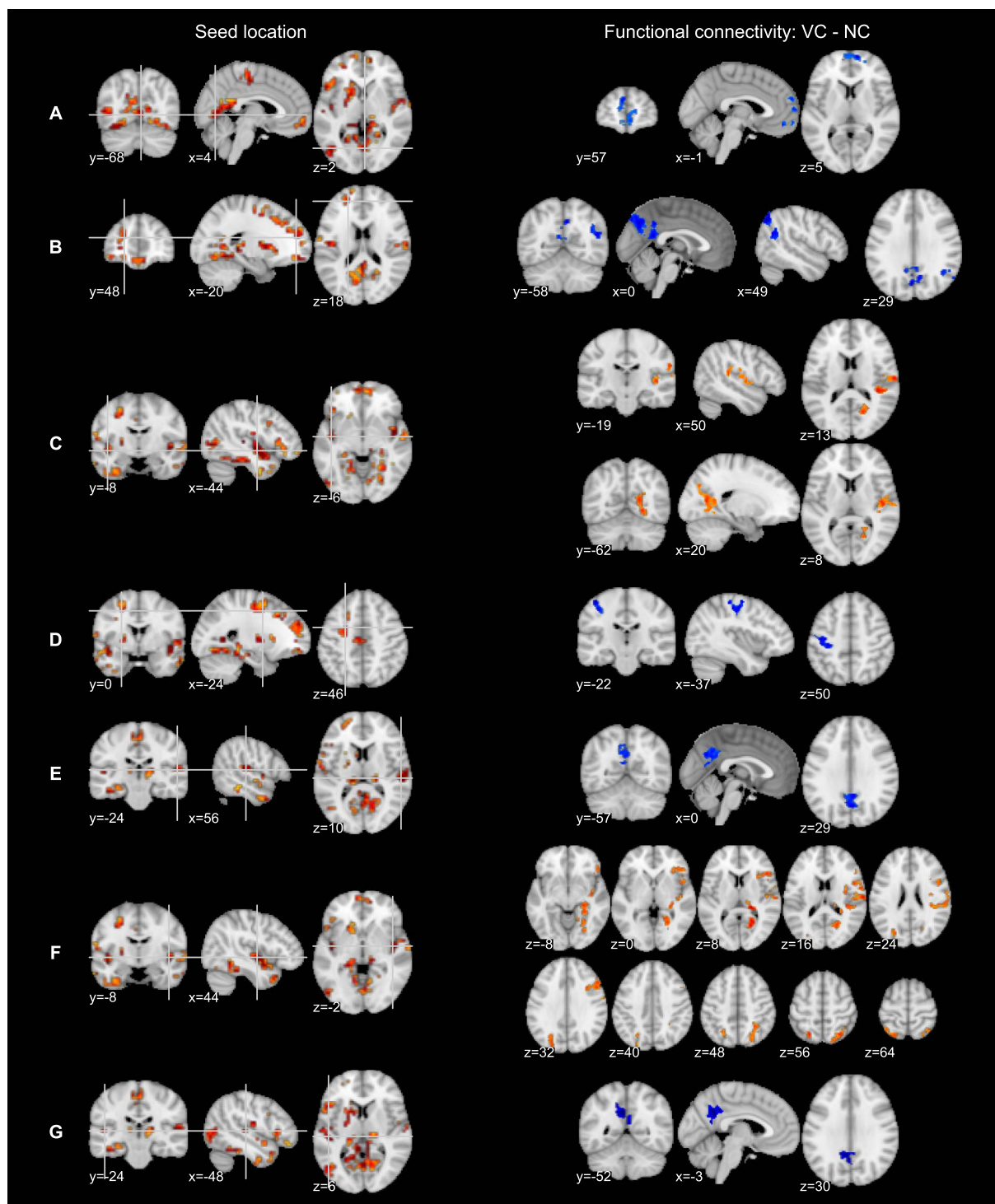
Fig. 4. Seed locations (indicated by crosshair) on the MDMR statistical map (left) and *t*-value maps of the regions with significantly (voxel-wise $p < 0.005$ and cluster-size-corrected $p < 0.016$) altered connectivity (right) for VC (veteran controls) compared to NC (non-trauma-exposed controls) in post-hoc analysis. Connectivity alteration for VC was found for seed locations at the left lingual gyrus (A), left superior frontal gyrus (B), left insula (C), left middle frontal gyrus (D), right transverse temporal gyrus (E), right insula (F), and left superior temporal gyrus (G).

connectivity alterations in Supplementary Figs. S2 and S3. Box plots of these figures show distribution of mean connectivity in the regions with significant alteration for PTSD (Supplementary Fig. S2) and VC (Supplementary Fig. S3) compared to NC. Supplementary Fig. S3 indicates that connectivity differences between VC and NC were not driven by the subjects with remitted morbidity. Supplementary Fig. S2 indicates that connectivity for VC tended to be in between PTSD and NC either with or without remitted morbidity, although variability in the

VC group could be increased by remitted morbidity. We further performed the same MDMR and post-hoc analyses excluding VC subjects with morbidity histories. This analysis, however, still did not show a significant connectivity difference between the PTSD and VC groups.

4. Discussion

Connectome-wide analysis of altered resting-state functional

connectivity for war veterans revealed decreased connectivity for PTSD patients in lateral frontal, SMA, and SN regions, as well as decreased connectivity between the parahippocampal and the visual cortex areas. PTSD symptom severity was negatively correlated with connectivity between the right parahippocampal gyrus and the right anterior insula and between the left vmPFC and the left middle frontal gyrus in people with PTSD. The analysis also revealed altered resting-state connectivity for VC, including increased connectivity in the posterior insula and decreased connectivity in the precuneus with several other brain areas, while no significant differences between PTSD and VC groups were observed. Because there was no significant difference in spatial smoothness or TSNR of functional images between veterans and NC groups, observed connectivity differences cannot be attributed to scan parameter difference. Most of these findings were consistent with previous observations of abnormal brain activation patterns among people with PTSD in both task-based and resting-state fMRI studies. The current results also extended previous findings by indicating such abnormalities were seen in region-by-region resting-state functional connectivity.

The analysis revealed decreased functional connectivity between the parahippocampal and the occipital visual cortex regions for PTSD compared to NC (Fig. 2A). A correlation between PTSD symptom severity and decreased functional connectivity between the para-hippocampal region and the anterior insula was also observed (Fig. 3A). Similar dissociation between the hippocampal memory area and sensorimotor and SN areas has been observed during PTSD-related flashbacks (Whalley et al., 2013). Whalley et al. (2013) indicated that PTSD patients showed hyperactive sensorimotor regions, including visual cortices and hypoactive memory-associated regions (e.g., parahippocampal gyrus), during a trauma cue-elicited flashback experience. This dissociation is consistent with the dual representation theory of PTSD (Brewin et al., 2010). According to the theory, episodic memory has dual representations of context (C-reps) supported by the medial temporal regions, and low-level sensation (S-reps) supported by sensory and interoceptive cortical areas. These representations are associated with each other for a memory of common events, while the C-reps for a memory of a traumatic event could be weakened or lost. This hypothesis is supported by evidence that potentiated amygdala function as well as suppressed hippocampal function was seen under high-level stress situations (Brewin et al., 2010; Elzinga and Bremner, 2002; Payne et al., 2006). The dual representation theory suggests that abnormal memory representation for a traumatic event has strong S-reps without associated C-reps, which underlies symptoms of re-experiencing and hyperarousal. The current results extended this evidence by indicating that resting-state functional connectivity between C-reps and S-reps regions was decreased in PTSD. This suggests that the neurobiological dissociation thought to underlie dual memory representations may be present at rest as well as during cued memory retrieval.

The current results also showed that the PTSD group had decreased functional connectivity across the lateral frontal areas and the SMA with the SN (Fig. 2B, D, E, F) as well as decreased connectivity between the vmPFC and the left middle frontal gyrus that was correlated with PTSD symptom severity (Fig. 3B). A large literature has indicated that lateral frontal regions, vmPFC, and SMA are associated with emotion regulation functions, including reappraisal of emotional stimuli (Johnstone et al., 2007; Kalisch, 2009; Kohn et al., 2014; New et al., 2009; Wager et al., 2008). Decreased activation of these regions in response to emotional stimuli or emotion regulation tasks among people with PTSD has been reported (Aupperle et al., 2012; Blair et al., 2013; Hayes et al., 2012; Patel et al., 2012; van Rooij et al., 2014). Yin et al. (2011) showed that resting-state ALFF at the right medial frontal gyrus was correlated with PTSD symptom severity. A meta-analysis of regional resting-state activation (Koch et al., 2016) also indicated lowered resting-state activity at the middle frontal gyrus for PTSD. In contrast to hypoactive prefrontal emotion-regulating areas, a hyperactive SN is one of the prevalent brain abnormalities observed among

people with PTSD in emotion-related tasks (Hayes et al., 2012; Lanius et al., 2015; Patel et al., 2012). A study of resting-state functional connectivity at the anterior insula (Sripada et al., 2012) also indicated that PTSD had increased anterior insula connectivity with SN regions but decreased connectivity with DMN regions, including the medial PFC. The current results of hypoconnectivity between the lateral prefrontal and SN regions are consistent with these previous reports of aberrant brain activations for PTSD.

Notably, the lowered functional connectivity of the lateral frontal areas was lateralized to the left hemisphere in the current results. Systematic review of brain activation patterns observed during cognitive reappraisal to regulate emotional experience among healthy individuals (Ochsner et al., 2012) suggested that there are two different tactics of reappraisal, reinterpretation and distancing. Their meta-analysis indicated that the regions involved in reinterpretation appear to be more strongly left-lateralized in prefrontal and temporal cortices, whereas regions involved in distancing appear to be more strongly right-lateralized in prefrontal cortex and parietal regions. The left-lateralized hypoconnectivity in the current results, therefore, might suggest that PTSD patients had reduced reinterpretation function compared to distancing. Distancing function, however, could be highly variable across PTSD patients. There is a subtype of PTSD patients with dissociation symptoms (Lanius et al., 2006; Lanius et al., 2005; Nicholson et al., 2015; Nicholson et al., 2016) who show depersonalization and derealization responses to emotional or trauma-related stimuli and could be involuntary distancing to regulate emotional arousal. In the current study, only 9 of the 35 PTSD subjects reported mild dissociation symptoms. Due to the small number of subjects and mild symptoms, we could not evaluate the difference between PTSD subtypes. Future studies are needed to examine differences in resting-state connectivity between subtypes of PTSD.

Increased functional connectivity at the posterior insula was observed among PTSD patients (Fig. 2.C) as well as among VC subjects (Fig. 4C, F) but in more areas for VC than PTSD. Similar differences in resting-state insula activity were reported in a meta-analysis of resting-state regional activity (Wang et al., 2016), which found that trauma-exposed controls had higher regional resting-state activity in the right posterior insula compared to people with PTSD. Zhang et al. (2016) reported hypoconnectivity in PTSD at the right posterior insula with the left inferior parietal lobe and the postcentral gyrus. A negative correlation between hyperarousal symptoms and connectivity between the posterior insula and the SN was also reported (Tursich et al., 2015), suggesting greater connectivity of the posterior insula is associated with lower PTSD symptom levels. Consistent with these findings, greater pretreatment insula gray matter density predicts better response to psychotherapy (Colvonen et al., 2017; Nardo et al., 2010). These findings suggest that greater functional connectivity and volume of the posterior insula could contribute to the alleviation of PTSD symptom. As the insula is thought to support internal representations of emotional states (Craig, 2003), the heightened activity and connectivity at this region might possibly help to accommodate internal emotional states of trauma experience.

Veteran controls also showed reduced connectivity at the precuneus (Fig. 4B, E, G). Patel et al. (2012) showed that the precuneus was hyperactive for PTSD, while most other DMN regions were hypoactive in PTSD in their meta-analysis of functional brain activation studies for PTSD. Cwik et al. (2016) also showed that for acute stress disorder patients the right medial precuneus response to trauma-related pictures was positively correlated with later development of PTSD symptoms. It has been suggested that the precuneus subserves consciousness and self-reflection (Vogt and Laureys, 2005). The dual representation theory (Brewin et al., 2010) suggests precuneus activity triggers top-down retrieval of S-reps with translation into a personally relevant (e.g. egocentric) perspective. It has also been suggested that decreased precuneus function is associated with efforts to terminate self-reflection of aversive sensations (Vogt and Laureys, 2005; Whalley et al., 2013). The

decreased connectivity at the precuneus for VC, therefore, might reflect effort to terminate self-reflection of aversive sensations, such as S-reps of traumatic memory.

Veteran controls also had decreased resting-state functional connectivity between the vmPFC and lingual gyrus (Fig. 4A) and between the left middle frontal and the left postcentral regions (Fig. 4D). It is possible that these reductions in connectivity are effects of traumatization and therefore are comparable to people with PTSD. Several remitted morbidities might also affect the alterations observed among VCs, although we did not observe systematic differences between VCs with and without remitted morbidity for these connectivity findings (Supplementary Fig. S3). It is possible that the abnormalities observed among VCs are due to war deployment, military training, or adaptive changes to traumatic experiences, or that they reflect an innate resilience factor. Future studies that employ longitudinal designs are needed to distinguish the cause of altered resting-state functional connectivity among war-deployed veterans without PTSD.

The current results did not show significant differences in resting-state functional connectivity between the PTSD and VC groups. We note that this result does not necessarily indicate that PTSD and VC groups had the same connectivity patterns. Statistically, a non-significant result does not mean equivalence of the groups. This non-significant result could be due to substantial variability in the VC group, which included individuals with remitted morbidity. However, even when we excluded VC subjects with morbidity history from the analysis, we still did not find significantly different connectivity between the PTSD and VC groups. This suggests that either morbidity history was not a sole reason for variability or that reduced statistical power due to smaller sample sizes negated the benefit of reducing variability within a group. Limited sensitivity of MDMR analysis, as discussed below, could also affect the non-significant result. Accordingly, we cannot draw inferences about the equivalence of the PTSD and VC groups based on this non-significant result, particularly in light of different patterns of connectivity alteration in the PTSD and VC groups compared to the NC group in the current results and previous research that demonstrated connectivity differences between people with PTSD and trauma-exposed controls.

Variability in morbidity and trauma is typical among war-deployed veterans. Even within PTSD patients, expression of the disorder is highly heterogeneous, making it difficult to find a single diagnostic marker of the disorder (Zoladz and Diamond, 2013). Importantly, the current results do not suggest homogeneous abnormality either for the PTSD or VC groups, but suggest average differences between groups. While such between-group designs continue to contribute to our limited understanding of the neuropathology of mental disorders, variability within a diagnostic group needs to be included in analyses in accord with the research domain criteria (RDoC) (Cuthbert, 2014) for further understanding the disorder.

It is also warranted to address a limitation of MDMR analysis. The current analysis did not observe a significant effect in the amygdala, where many studies have indicated abnormality in PTSD (Shin et al., 2006). Whole-brain analyses often do not observe abnormalities in amygdala activity, whereas region of interest (ROI) analyses do observe such abnormalities (Hayes et al., 2012). A meta-analysis (Hayes et al., 2012) including only whole-brain analyses did not find amygdala abnormality for PTSD, while an analysis including ROI analyses found amygdala hyperactivity for PTSD. One reason for the absence of amygdala abnormalities in the current results, therefore, could be its small effect size. Limited sensitivity of MDMR analysis, however, could also be a reason for this result. MDMR analysis evaluates between-subject distance of connectivity maps, and this distance measure could be insensitive to a change in a small region because it summarizes the differences in a large dimensional connectivity map into one measure. Non-significant results in MDMR, therefore, should not be interpreted as indication of a negative result. The distance measure of the MDMR also introduces another limitation, that is, a distance measure reflects only a size of difference and is not sensitive to how connectivity maps differ. This means that a similar distance value could come from different patterns of connectivity alteration. As the current results demonstrated that not all the seed locations identified with MDMR showed significant group differences in the post-hoc analysis, significant group effects in the MDMR do not necessarily indicate common differences in the group. Post-hoc analysis that investigates what differences contribute to the MDMR measure is needed for correct interpretation of MDMR results.

5. Conclusions

Connectome-wide investigation of altered resting-state functional connectivity for war veterans with PTSD revealed hypoconnectivity between the parahippocampus gyrus and the visual cortex as well as across the lateral prefrontal and vmPFC with the SN regions. These alterations were consistent with previous observations of abnormalities in the emotion-regulation circuit and further support dissociated memory representation in PTSD. The current results extended these findings by indicating that such abnormality also appears to be present in resting-state region-by-region functional connectivity. The analysis also revealed increased connectivity with posterior insula and decreased connectivity with precuneus among veterans without PTSD, with the later suggesting adaptive alteration to suppress traumatic memory. While all the reasons for these observed alterations are not yet clear, the comprehensive exploration via MDMR analysis enabled these findings and offers potential targets for future research. Although we should recognize limitations in sensitivity and interpretation, hypothesis-free exploratory analysis with MDMR connectome-wide investigation yielded valuable information that complements existing hypothesis-driven analyses.

Appendix A. Supplementary data

Supplementary data to this article can be found online at https://doi.org/10.1016/j.nicl.2017.10.032.

References

American Psychiatric Association, 2000. Diagnostic and Statistical Manual of Mental Disorders DSM-IV-TR, Fourth edition. American Psychiatric Publishing, Washington, DC (Text Revision).

Anderson, M.J., 2001. A new method for non-parametric multivariate analysis of variance. Austral Ecol. 26, 32–46.

Aupperle, R.L., Melrose, A.J., Stein, M.B., Paulus, M.P., 2012. Executive function and PTSD: disengaging from trauma. Neuropharmacology 62, 686–694.

Avants, B.B., Epstein, C.L., Grossman, M., Gee, J.C., 2008. Symmetric diffeomorphic image registration with cross-correlation: evaluating automated labeling of elderly and neurodegenerative brain. Med. Image Anal. 12, 26–41.

Birn, R.M., Smith, M.A., Jones, T.B., Bandettini, P.A., 2008. The respiration response function: the temporal dynamics of fMRI signal fluctuations related to changes in respiration. NeuroImage 40, 644–654.

Blair, K., Vythilingam, M., Crowe, S., McCaffrey, D., Ng, P., Wu, C., Scaramozza, M., Mondillo, K., Pine, D., Charney, D., 2013. Cognitive control of attention is differentially affected in trauma-exposed individuals with and without post-traumatic stress disorder. Psychol. Med. 43, 85–95.

Blake, D., Weathers, F., Nagy, L., Kaloupek, D., Charney, D., Keane, T., 1995. Clinician-Administered PTSD Scale for DSM-IV (CAPS-DX). National Center for Posttraumatic Stress Disorder, Behavioral Science Division, Boston VA Medical Center, Boston, MA.

Blanchard, E.B., Jones-Alexander, J., Buckley, T.C., Forneris, C.A., 1996. Psychometric properties of the PTSD checklist (PCL). Behav. Res. Ther. 34, 669–673.

Bonne, O., Gilboa, A., Louzoun, Y., Brandes, D., Yona, I., Lester, H., Barkai, G., Freedman, N., Chisin, R., Shalev, A.Y., 2003. Resting regional cerebral perfusion in recent posttraumatic stress disorder. Biol. Psychiatry 54, 1077–1086.

Brewin, C.R., 2011. The nature and significance of memory disturbance in posttraumatic stress disorder. Annu. Rev. Clin. Psychol. 7, 203–227.

Brewin, C.R., Gregory, J.D., Lipton, M., Burgess, N., 2010. Intrusive images in psychological disorders: characteristics, neural mechanisms, and treatment implications. Psychol. Rev. 117, 210–232.

Brown, V.M., LaBar, K.S., Haswell, C.C., Gold, A.L., McCarthy, G., Morey, R.A., 2014. Altered resting-state functional connectivity of basolateral and centromedial amygdala complexes in posttraumatic stress disorder. Neuropsychopharmacology 39, 351–359.

Calhoun, V.D., Adali, T., 2012. Multisubject independent component analysis of fMRI: a decade of intrinsic networks, default mode, and neurodiagnostic discovery. IEEE Rev. Biomed. Eng. 5, 60–73.

Colvonen, P.J., Glassman, L.H., Crocker, L.D., Buttner, M.M., Orff, H., Schiehser, D.M., Norman, S.B., Afari, N., 2017. Pretreatment biomarkers predicting PTSD psychotherapy outcomes: a systematic review. Neurosci. Biobehav. Rev. 75, 140–156.

Craig, A.D., 2003. Interoception: the sense of the physiological condition of the body. Curr. Opin. Neurobiol. 13, 500–505.

Cuthbert, B.N., 2014. The RDoC framework: facilitating transition from ICD/DSM to dimensional approaches that integrate neuroscience and psychopathology. World Psychiatry 13, 28–35.

Cwik, J.C., Sartory, G., Nuyken, M., Schürholt, B., Seitz, R.J., 2016. Posterior and prefrontal contributions to the development posttraumatic stress disorder symptom severity: an fMRI study of symptom provocation in acute stress disorder. Eur. Arch. Psychiatry Clin. Neurosci. 1–11.

Eklund, A., Nichols, T.E., Knutsson, H., 2016. Cluster failure: why fMRI inferences for spatial extent have inflated false-positive rates. Proc. Natl. Acad. Sci. U. S. A. 113, 7900–7905.

Elzinga, B.M., Bremner, J.D., 2002. Are the neural substrates of memory the final common pathway in posttraumatic stress disorder (PTSD)? J. Affect. Disord. 70, 1–17.

Filippini, N., MacIntosh, B.J., Hough, M.G., Goodwin, G.M., Frisoni, G.B., Smith, S.M., Matthews, P.M., Beckmann, C.F., Mackay, C.E., 2009. Distinct patterns of brain activity in young carriers of the APOE-epsilon4 allele. Proc. Natl. Acad. Sci. U. S. A. 106, 7209–7214.

First, M.B., Spitzer, R.L., Miriam, G., Williams, J.B.W., 1996. Structured Clinical Interview for DSM-IV Axis I Disorders, Clinician Version (SCID-CV). American Psychiatric Press, Inc., Washington, D.C.

Fonzo, G.A., Simmons, A.N., Thorp, S.R., Norman, S.B., Paulus, M.P., Stein, M.B., 2010. Exaggerated and disconnected insular-amygdalar blood oxygenation level-dependent response to threat-related emotional faces in women with intimate-partner violence posttraumatic stress disorder. Biol. Psychiatry 68, 433–441.

Fornito, A., Zalesky, A., Breakspear, M., 2013. Graph analysis of the human connectome: promise, progress, and pitfalls. NeuroImage 80, 426–444.

Friedman, L., Glover, G.H., 2006. Reducing interscanner variability of activation in a multicenter fMRI study: controlling for signal-to-fluctuation-noise-ratio (SFNR) differences. NeuroImage 33, 471–481.

Friedman, L., Glover, G.H., Krenz, D., Magnotta, V., 2006. Reducing inter-scanner variability of activation in a multicenter fMRI study: role of smoothness equalization. NeuroImage 32, 1656–1668.

Friston, K., 1994. Functional and effective connectivity in neuroimaging: a synthesis. Hum. Brain Mapp. 2, 56–78.

Glover, G.H., Li, T.Q., Ress, D., 2000. Image-based method for retrospective correction of physiological motion effects in fMRI: RETROICOR. Magn. Reson. Med. 44, 162–167.

Hamilton, M., Schutte, N., Malouff, J., 1976. Hamilton anxiety scale (HAMA). Sourcebook of adult assessment: applied clinical. Psychology 154–157.

Hayes, J.P., Hayes, S.M., Mikedis, A.M., 2012. Quantitative meta-analysis of neural activity in posttraumatic stress disorder. Biol. Mood Anxiety Disord. 2, 1–13.

Hoge, C.W., Auchterlonie, J.L., Milliken, C.S., 2006. Mental health problems, use of mental health services, and attrition from military service after returning from deployment to Iraq or Afghanistan. JAMA 295, 1023–1032.

Jiang, Q., Ahmed, S., 2009. An analysis of correlations among four outcome scales employed in clinical trials of patients with major depressive disorder. Ann. General Psychiatry 8, 4.

Jo, H.J., Saad, Z.S., Simmons, W.K., Milbury, L.A., Cox, R.W., 2010. Mapping sources of correlation in resting state FMRI, with artifact detection and removal. NeuroImage 52, 571–582.

Johnstone, T., van Reekum, C.M., Urry, H.L., Kalin, N.H., Davidson, R.J., 2007. Failure to regulate: counterproductive recruitment of top-down prefrontal-subcortical circuitry in major depression. J. Neurosci. 27, 8877–8884.

Kalisch, R., 2009. The functional neuroanatomy of reappraisal: time matters. Neurosci. Biobehav. Rev. 33, 1215–1226.

Kennis, M., Rademaker, A.R., van Rooij, S.J., Kahn, R.S., Geuze, E., 2015. Resting state functional connectivity of the anterior cingulate cortex in veterans with and without post-traumatic stress disorder. Hum. Brain Mapp. 36, 99–109.

Koch, S.B., van Zuiden, M., Nawijn, L., Frijling, J.L., Veltman, D.J., Olff, M., 2016. Aberrant resting-state brain activity in posttraumatic stress disorder: a meta-analysis and systematic review. Depress. Anxiety 33, 592–606.

Kohn, N., Eickhoff, S.B., Scheller, M., Laird, A.R., Fox, P.T., Habel, U., 2014. Neural network of cognitive emotion regulation–an ALE meta-analysis and MACM analysis. NeuroImage 87, 345–355.

Lanius, R.A., Williamson, P.C., Bluhm, R.L., Densmore, M., Boksman, K., Neufeld, R.W., Gati, J.S., Menon, R.S., 2005. Functional connectivity of dissociative responses in posttraumatic stress disorder: a functional magnetic resonance imaging investigation.

Biol. Psychiatry 57, 873–884.

Lanius, R.A., Bluhm, R., Lanius, U., Pain, C., 2006. A review of neuroimaging studies in PTSD: heterogeneity of response to symptom provocation. J. Psychiatr. Res. 40, 709–729.

Lanius, R.A., Frewen, P.A., Tursich, M., Jetly, R., McKinnon, M.C., 2015. Restoring large-scale brain networks in PTSD and related disorders: a proposal for neuroscientifically-informed treatment interventions. Eur. J. Psychotraumatol. 6, 27313.

Lei, D., Li, K., Li, L., Chen, F., Huang, X., Lui, S., Li, J., Bi, F., Gong, Q., 2015. Disrupted functional brain connectome in patients with posttraumatic stress disorder. Radiology 276, 818–827.

Liberzon, I., Sripada, C.S., 2008. The functional neuroanatomy of PTSD: a critical review. Prog. Brain Res. 167, 151–169.

Maier, W., Buller, R., Philipp, M., Heuser, I., 1988. The Hamilton Anxiety Scale: reliability, validity and sensitivity to change in anxiety and depressive disorders. J. Affect. Disord. 14, 61–68.

Menon, V., Uddin, L.Q., 2010. Saliency, switching, attention and control: a network model of insula function. Brain Struct. Funct. 214, 655–667.

Misaki, M., Suzuki, H., Savitz, J., Drevets, W.C., Bodurka, J., 2016. Individual variations in nucleus accumbens responses associated with major depressive disorder symptoms. Sci Rep 6, 21227.

Montgomery, S.A., Asberg, M., 1979. A new depression scale designed to be sensitive to change. Br. J. Psychiatry 134, 382–389.

Nardo, D., Hogberg, G., Looi, J.C., Larsson, S., Hallstrom, T., Pagani, M., 2010. Gray matter density in limbic and paralimbic cortices is associated with trauma load and EMDR outcome in PTSD patients. J. Psychiatr. Res. 44, 477–485.

New, A.S., Fan, J., Murrough, J.W., Liu, X., Liebman, R.E., Guise, K.G., Tang, C.Y., Charney, D.S., 2009. A functional magnetic resonance imaging study of deliberate emotion regulation in resilience and posttraumatic stress disorder. Biol. Psychiatry 66, 656–664.

Nicholson, A.A., Densmore, M., Frewen, P.A., Theberge, J., Neufeld, R.W., McKinnon, M.C., Lanius, R.A., 2015. The dissociative subtype of posttraumatic stress disorder: unique resting-state functional connectivity of basolateral and centromedial amygdala complexes. Neuropsychopharmacology 40, 2317–2326.

Nicholson, A.A., Sapru, I., Densmore, M., Frewen, P.A., Neufeld, R.W., Theberge, J., McKinnon, M.C., Lanius, R.A., 2016. Unique insula subregion resting-state functional connectivity with amygdala complexes in posttraumatic stress disorder and its dissociative subtype. Psychiatry Res. 250, 61–72.

Ochsner, K.N., Silvers, J.A., Buhle, J.T., 2012. Functional imaging studies of emotion regulation: a synthetic review and evolving model of the cognitive control of emotion. Ann. N. Y. Acad. Sci. 1251, E1–24.

Patel, R., Spreng, R.N., Shin, L.M., Girard, T.A., 2012. Neurocircuitry models of posttraumatic stress disorder and beyond: a meta-analysis of functional neuroimaging studies. Neurosci. Biobehav. Rev. 36, 2130–2142.

Payne, J.D., Jackson, E.D., Ryan, L., Hoscheidt, S., Jacobs, J.W., Nadel, L., 2006. The impact of stress on neutral and emotional aspects of episodic memory. Memory 14, 1–16.

Pitman, R.K., Rasmusson, A.M., Koenen, K.C., Shin, L.M., Orr, S.P., Gilbertson, M.W., Milad, M.R., Liberzon, I., 2012. Biological studies of post-traumatic stress disorder. Nat. Rev. Neurosci. 13, 769–787.

Power, J.D., Schlaggar, B.L., Petersen, S.E., 2015. Recent progress and outstanding issues in motion correction in resting state fMRI. NeuroImage 105, 536–551.

Reimherr, F.W., Martin, M.L., Eudicone, J.M., Marchant, B.K., Tran, Q.V., Pikalov, A., Marcus, R.N., Berman, R.M., Carlson, B.X., 2010. A pooled MADRS/IDS cross-correlation analysis: clinician and patient self-report assessment of improvement in core depressive symptoms with adjunctive aripiprazole. J. Clin. Psychopharmacol. 30, 300–305.

Ruggiero, K.J., Del Ben, K., Scotti, J.R., Rabalais, A.E., 2003. Psychometric properties of the PTSD checklist-civilian version. J. Trauma. Stress. 16, 495–502.

Satterthwaite, T.D., Cook, P.A., Bruce, S.E., Conway, C., Mikkelsen, E., Satchell, E., Vandekar, S.N., Durbin, T., Shinohara, R.T., Sheline, Y.I., 2015. Dimensional depression severity in women with major depression and post-traumatic stress disorder correlates with fronto-amygdalar hypoconnectivty. Mol. Psychiatry 21, 894–902.

Shehzad, Z., Kelly, C., Reiss, P.T., Cameron Craddock, R., Emerson, J.W., McMahon, K., Copland, D.A., Castellanos, F.X., Milham, M.P., 2014. A multivariate distance-based analytic framework for connectome-wide association studies. NeuroImage 93 (Pt 1), 74–94.

Shin, L.M., Rauch, S.L., Pitman, R.K., 2006. Amygdala, medial prefrontal cortex, and hippocampal function in PTSD. Ann. N. Y. Acad. Sci. 1071, 67–79.

Sripada, R.K., King, A.P., Welsh, R.C., Garfinkel, S.N., Wang, X., Sripada, C.S., Liberzon, I., 2012. Neural dysregulation in posttraumatic stress disorder: evidence for disrupted equilibrium between salience and default mode brain networks. Psychosom. Med. 74, 904–911.

Tursich, M., Ros, T., Frewen, P.A., Kluetsch, R.C., Calhoun, V.D., Lanius, R.A., 2015. Distinct intrinsic network connectivity patterns of post-traumatic stress disorder symptom clusters. Acta Psychiatr. Scand. 132, 29–38.

van Rooij, S.J., Rademaker, A.R., Kennis, M., Vink, M., Kahn, R.S., Geuze, E., 2014. Impaired right inferior frontal gyrus response to contextual cues in male veterans with PTSD during response inhibition. J. Psychiatry Neurosci. 39, 330–338.

van Wingen, G.A., Geuze, E., Caan, M.W., Kozicz, T., Olabarriaga, S.D., Denys, D., Vermetten, E., Fernandez, G., 2012. Persistent and reversible consequences of combat stress on the mesofrontal circuit and cognition. Proc. Natl. Acad. Sci. U. S. A. 109, 15508–15513.

Vogt, B.A., Laureys, S., 2005. Posterior cingulate, precuneus and retrosplenial cortices: cytology and components of the neural network correlates of consciousness. Prog. Brain Res. 150, 205–217.

Wager, T.D., Davidson, M.L., Hughes, B.L., Lindquist, M.A., Ochsner, K.N., 2008.

Prefrontal-subcortical pathways mediating successful emotion regulation. Neuron 59, 1037–1050.

Wang, T., Liu, J., Zhang, J., Zhan, W., Li, L., Wu, M., Huang, H., Zhu, H., Kemp, G.J., Gong, Q., 2016. Altered resting-state functional activity in posttraumatic stress disorder: a quantitative meta-analysis. Sci Rep 6, 27131.

Weathers, F.W., Litz, B.T., Herman, D.S., Huska, J.A., Keane, T.M., 1993. The PTSD Checklist (PCL): reliability, validity, and diagnostic utility. In: Annual Convention of the International Society for Traumatic Stress Studies, (San Antonio, TX).

Weathers, F.W., Keane, T.M., Davidson, J.R., 2001. Clinician-administered PTSD scale: a review of the first ten years of research. Depress. Anxiety 13, 132–156.

Whalley, M.G., Kroes, M.C., Huntley, Z., Rugg, M.D., Davis, S.W., Brewin, C.R., 2013. An fMRI investigation of posttraumatic flashbacks. Brain Cogn. 81, 151–159.

Winkler, A.M., Ridgway, G.R., Webster, M.A., Smith, S.M., Nichols, T.E., 2014. Permutation inference for the general linear model. NeuroImage 92, 381–397.

Yin, Y., Li, L., Jin, C., Hu, X., Duan, L., Eyler, L.T., Gong, Q., Song, M., Jiang, T., Liao, M., Zhang, Y., Li, W., 2011. Abnormal baseline brain activity in posttraumatic stress disorder: a resting-state functional magnetic resonance imaging study. Neurosci. Lett. 498, 185–189.

Zang, Y., Jiang, T., Lu, Y., He, Y., Tian, L., 2004. Regional homogeneity approach to fMRI data analysis. NeuroImage 22, 394–400.

Zhang, Y., Xie, B., Chen, H., Li, M., Guo, X., Chen, H., 2016. Disrupted resting-state insular subregions functional connectivity in post-traumatic stress disorder. Medicine (Baltimore) 95, e4083.

Zhu, H., Qiu, C., Meng, Y., Cui, H., Zhang, Y., Huang, X., Zhang, J., Li, T., Gong, Q., Zhang, W., Lui, S., 2015. Altered spontaneous neuronal activity in chronic post-traumatic stress disorder patients before and after a 12-week paroxetine treatment. J. Affect. Disord. 174, 257–264.

Zoladz, P.R., Diamond, D.M., 2013. Current status on behavioral and biological markers of PTSD: a search for clarity in a conflicting literature. Neurosci. Biobehav. Rev. 37, 860–895.

Zou, Q.H., Zhu, C.Z., Yang, Y., Zuo, X.N., Long, X.Y., Cao, Q.J., Wang, Y.F., Zang, Y.F., 2008. An improved approach to detection of amplitude of low-frequency fluctuation (ALFF) for resting-state fMRI: fractional ALFF. J. Neurosci. Methods 172, 137–141.